Numerical modelling of creep in soft soils

Modélisation numérique du fluage en sols meubles

Martino Leoni
Wechselwirkung Numerische Geotechnik Studio Italiano, Italy

Pieter A. Vermeer
Institute of Geotechnical Engineering, University of Stuttgart

ABSTRACT

A new constitutive model for time-dependent behaviour of soft soils has been recently proposed. Stemming from a previously developed viscoelastic isotropic model based on ellipses of Modified Cam Clay, anisotropy was taken into account by introducing a fabric tensor to represent the rotation of the constitutive ellipses in p'-q (mean effective stress-deviatoric stress) plane. Due to the particle orientation induced by deposition mechanism, natural soils are anisotropic in terms of strength and stiffness. The improvement induced by the new formulation is particularly evident in stress paths in extension. The new soil constants required by the anisotropic formulation need no calibration, since they can be expressed in terms of parameters already used in the isotropic model and familiar to practicing geotechnical engineers. In this paper, the numerical analysis of an embankment on soft soils has been carried out, in order to investigate on the differences in terms of predictions of vertical and horizontal displacements between the isotropic and the anisotropic creep model.

RÉSUMÉ

Un nouveau modèle anisotrope pour le comportement des sols meubles en fonction du temps est présenté. Cette formulation est basée sur un modèle de fluage isotrope développé précédemment avec l'hypothèse que le Modified Cam Clay devient elliptique sous forme de courbes de niveau de vitesse de déformation volumétrique. Une loi d'écrouissage rotatoire est appliquée afin de prendre en compte les changements en anisotropie dus aux déformations visqueuses. Bien que cela introduise de nouveaux paramètres relatifs au sol, ceux-ci ne nécessitent aucune calibration car ils peuvent être exprimés comme des fonctions de paramètres de base du sol à l'aide d'expressions analytiques simples. La comparaison avec des données expérimentales montre une bonne adéquation en particulier pour extensions triaxiales en conditions non drainées. Dans la présente communication les différences entre formulation isotrope et anisotrope sont présentées en forme de déformations horizontales et verticales pour un remblai theoretique.

Keywords : creep, anisotropy, constitutive modelling, numerical modelling

1 INTRODUCTION

When dealing with soft soils, geotechnical engineers have become aware of the need of considering time-dependent behaviour of soft soils in order to improve design and guarantee stability and serviceability for the whole life of a structure. Researchers started to address the study of soft soils since the beginning of last Century.

To begin with, simple formulae resulting from the integration of the governing differential equations were proposed, allowing the solution of simple problems, or situations which could be reduced to simpler ones by means of simplifying assumptions. The validity of the isotache concept introduced by Suklje (1957) was confirmed by many experimental studies, and the concept was incorporated in empirical creep laws.

A major step forward was the introduction of the so-called overstress concept (Malvern 1951; Perzyna 1966) which led to a new generation of three dimensional creep models crossing the frontier of one dimensional theories. Firstly, ellipses of Modified Cam Clay were assumed as boundary between purely elastic and elasto-viscous region as postulated in Perzyna's overstress model.

Later on, it became clear that isotropic ellipses of Modified Cam Clay are inadequate for capturing the real stress-strain-time behaviour. New generations of anisotropic creep models were introduced (e.g. Sekiguchi & Ohta 1977), but anisotropy was mostly formulated as an initial rotation of constitutive ellipses which stay fixed notwithstanding the development of creep strains.

Within this scenario, in the late '90s an isotropic creep model was developed by Vermeer and coworkers (Vermeer & Neher 1999). Due to the model formulation it is possibile to reach states above the normal consolidation line when the load is applied in a short time, similarly to the overstress models.

However, in contrast, creep strains develop also inside the apparent yield surface, therefore excluding the presence of a purely elastic region. A smooth transition between mainly elastic (for overconsolidated states) and viscoelastic region is therefore achieved. The model was validated through comparison with laboratory tests and more complex boundary value problems. The model performance was good, and after its implementation into a commercial finite element code it has been widely used for geotechnical design.

The original isotropic creep model has been then enhanced to an anisotropic formulation, using the fabric tensor approach put forward by Wheeler et al. (2003) for the anisotropic elastoplastic model S-CLAY1. As in its elastoplastic counterpart, the new anisotropic creep model has been completed by introducing a rotational hardening law describing the evolution of anisotropy with volumetric and deviatoric creep strain rates (Leoni et al. 2008). The improvement introduced with the anisotropic formulation was confirmed by the results obtained when modelling shearing in triaxial extension starting from a K_0-consolidated state. In general, major differences occur whenever a large rotation of the fabric tensor is induced by creep strains.

In this paper, the comparison is extended to a more complex boundary value problem, i.e. an embankment resting on a thick layer of soft clays. Results are compared in terms of vertical and

Proceedings of the 17th International Conference on Soil Mechanics and Geotechnical Engineering
M. Hamza et al. (Eds.)

doi:10.3233/978-1-60750-031-5-578

horizontal displacements in different areas of the finite element model, thus showing the implications of the new formulation when applying it to real geotechnical engineering problems.

The first part of the paper describes the general framework in which the anisotropic creep model is formulated. In further Sections the geometry of the finite element model of the embankment is described and results of the calculations are presented.

2 ANISOTROPIC CREEP MODEL

The description of the isotropic creep model on which the anisotropic formulation is based is not repeated here, as the interested reader can refer to previous publications (Vermeer & Neher 1999). Hence, this Section is focused on the new features introduced in the Anisotropic Creep Model, henceforth referred to as ACM.

The elastic and creep parts are combined with an additive law expressing the total strain rate as combination of elastic and creep component, analogous to classical elastoplasticity.

With the aim of achieving a better match with experimental data, a fabric tensor was included in the formulation. If the stress state is cross-anisotropic, with no rotation of principal directions during the test, anisotropy can be represented by a scalar parameter. In the triaxial stress state in which the tests have been performed, the constitutive ellipses are rotated in p'-q invariants plane by an angle expressed by the scalar α (Figure 1).

The first rotated ellipse defines the normal consolidation surface (NCS). The intersection of the vertical tangent to the ellipse with p' axis is the isotropic preconsolidation pressure p'_p. The size of this ellipse increases with volumetric creep strains according to the hardening law formulated in integrated form as:

$$p'_p = p'_{po} \cdot \exp\left(\frac{\varepsilon^c_{vol}}{\lambda^* - \kappa^*}\right) \tag{1}$$

where λ^* and $\kappa^* \sigma'_{ij}$ are the modified compression and swelling indexes, respectively and e_0 is the initial void ratio. In Equation (1) soil mechanics sign convention is used, therefore compression is positive. A second curve is the ellipse passing through the point, representing the actual effective stress (Figure 1), called the current stress surface (CSS). The intersection of this second curve with the horizontal axis is the so-called equivalent mean stress. The equivalent mean stress can be regarded as an isotropic measure of the current stress and it is evaluated in closed form as:

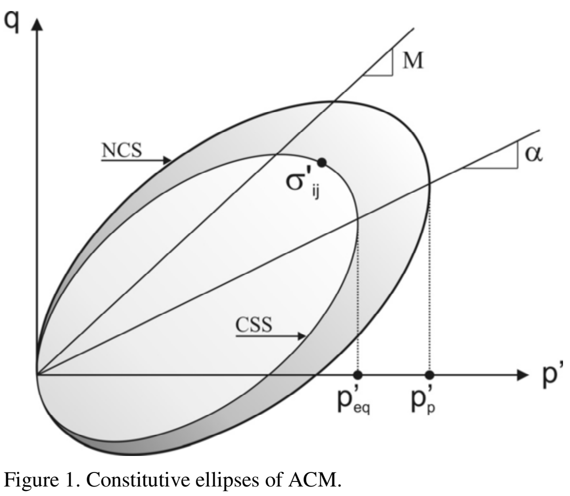

Figure 1. Constitutive ellipses of ACM.

$$p'_{eq} = p' + \frac{(q - \alpha \cdot p')^2}{\left(M^2 - \alpha^2\right) \cdot p'} \tag{2}$$

where M is the stress ratio at critical state. The ratio between preconsolidation pressure and equivalent stress is then assumed as the isotropic overconsolidation ratio OCR^*, being a measure on the isotropic axis of the distance between the current stress and the preconsolidation pressure.

The volumetric creep strain rate is given by the power law

$$\dot{\varepsilon}^c_{vol} = \frac{\mu^*}{\tau}\left(\frac{1}{OCR^*}\right)^{\beta} \quad \text{where} \quad \mu^* = \frac{C_\alpha}{\ln 10\,(1 + e_o)} \tag{3}$$

where μ^* is referred to as modified creep index, and τ is the so-called reference time that is set to 24h if the NCS is found performing a standard 24h oedometer test. For further details, the interested reader is referred to Leoni et al. 2008. The deviatoric component of the creep strain rate vector results simply from the flow rule, which for the sake of simplicity is assumed as associated. The scalar quantity α in Equation (2) acts like a rotational hardening parameter, and its evolution is governed by creep strains according to a simple rotational hardening law (Leoni et al. 2008 for details).

The mechanism of generation of creep strains is analogous to the one of overstress models, with the fundamental difference that in ACM creep strains are generated also in the overconsolidated range, even though the creep rate decreases exponentially with increasing OCR values.

The elastic part of the model is formulated in terms of generalized Hooke's law with stress dependent stiffness.

Although in Leoni et al. 2008 an extensive study of the effect of anisotropy in triaxial compression and extension tests is given, here it is focused on triaxial extension tests results. The specimens subjected to numerical simulations were first consolidated following the K_0^{NC} line and then subjected to

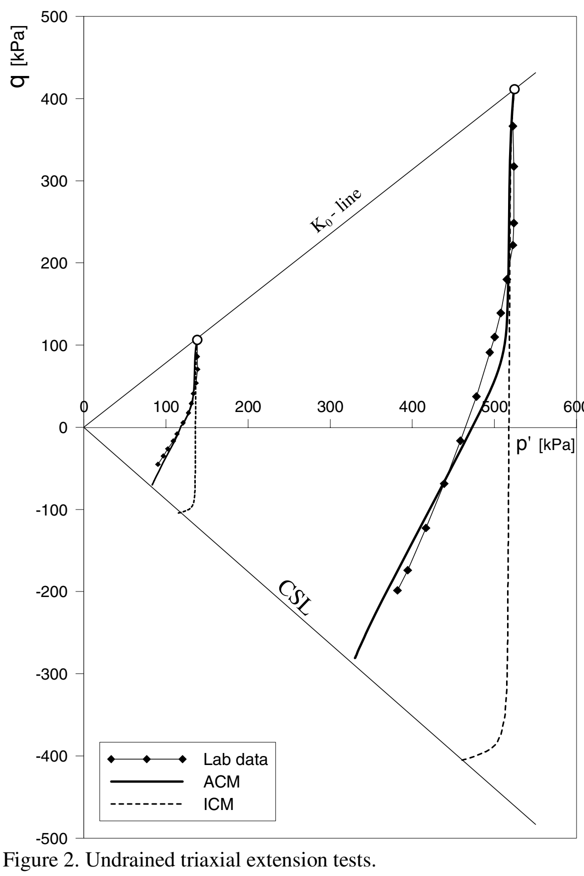

Figure 2. Undrained triaxial extension tests.

Table 1. Input parameters for isotropic (ICM) and anisotropic (ACM) creep models.

φ'	c'	ψ	ν	λ^*	κ^*	μ^*
[°]	[kPa]	[°]	[-]	[-]	[-]	[-]
30	0	0	0.2	0.24	0.01	0.0033

undrained triaxial shearing at an axial strain rate of 2%/hour. The comparisons between predicted and experimental results are plotted in Figure 2. The anisotropic model is in good agreement with the experiments, even if the final effective mean stress is larger (as absolute value) than the one measured in the laboratory. The inclination of the path is well captured, and if one were to prolongue the experimental test until the critical state is reached, the predicted undrained shear strength would match the measured one.

On the contrary, the isotropic model shows its inadequacy when modelling undrained extension tests. As shown in Figure 2, the (mainly) elastic region is too large and only when the stress path is already close to critical state p' starts to decrease towards the critical state line. Moreover, the undrained shear strength is clearly exceeded.

3 BENCHMARK EMBANKMENT

3.1 *Finite element model*

In order to evaluate the performance of the anisotropic creep model it was decided to analyse a complex boundary value problem simulating a real geotechnical engineering case.

Recently, an application of ACM was carried out in order to assess the capabilities of the model in to capture the stress-strain-time behaviour of silty soils of Venice lagoon (Berengo et al. 2008). The study showed the good predictions obtained in terms of predicted vertical and horizontal displacements.

The aim of this paper is to fully explore and understand the differences induced by anisotropy. The analysis considers a theoretical benchmark case. On doing so, the clear advantage is that one can focus on a key set of aspects, thus enabling a better understanding of the differences stemming from the different constitutive assumptions. The finite element analysis was considering an idealized embankment constructed on a material with properties of the so-called POKO clay (Koskinen et al. 2002).

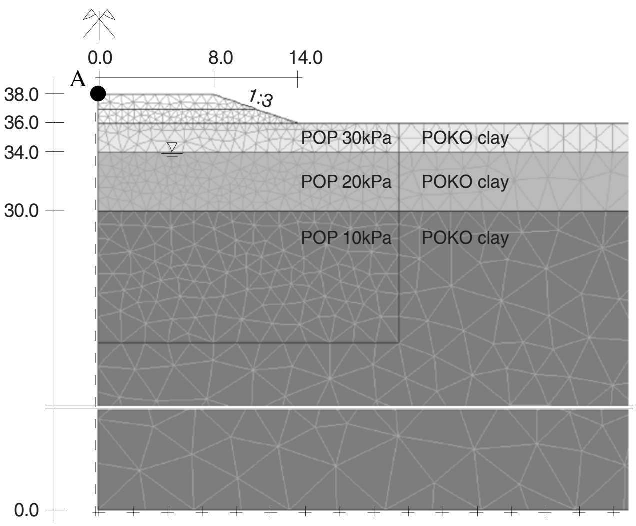

Figure 3. Geometry of the embankment and soil profile.

The subsoil was assumed to be homogeneous, with an overconsolidation ratio decreasing with depth via the definition of three distinct layers with varying vertical pre-overburden pressure (POP).

Considering that the deformation of the embankment is not relevant for the purposes of the present study, the embankment fill was modelled by using the elastic perfectly plastic Mohr-Coulomb model with a unit weight of 20 kN/m^3, Young modulus E'=40000 kPa, Poisson's ratio ν'=0.3, effective friction angle ϕ'=38°. Cohesion and dilatancy angle were set to zero. The groundwater table was assumed to be located 2 m below ground surface. Above water table, drained conditions and zero initial pore pressures were assumed. As far as the subsoil is concerned, the new anisotropic model ACM and the former isotropic version ICM were used. As for the initial condition, for both analyses the soil was assumed to be K_0-consolidated, with values for the lateral earth pressure at rest for a normally consolidated state in agreement with Jaky's formula (K_0 = 0.5). The model geometry of the benchmark embankment is shown in Figure 3. The vertical stress distribution was estimated by assuming a bulk unit weight of 15 kN/m^3. Material parameters of the creep models are given in Table 1. The analysis was performed using small deformations assumption. The construction of the embankment was simu-lated in two undrained phases (10 days each).

The first construction phase, in which the first layer of the embankment was built, was followed by a consolidation stage of 30 days. After the completion of the construction up to the final embankment height of 2 metres, a final consolidation phase of 100 years was simulated.

3.2 *Results of numerical analysis*

In this section results of numerical analysis are presented in terms of time-settlement curves, generated excess pore pressures and horizontal displacements (after construction and after 100 years of consolidation). The two constitutive models used for the subsoil differ only for the fact that in ICM the current stress surface and the normal consolidation surface are symmetric with respect to p' axis and stay fixed throughout the analysis. Both analyses assume the same initial state. Differences between results are therefore uniquely to be attributed to initial anisotropy and its evolution due to creep strains.

In Figure 4a results are presented in terms of vertical displacements versus time at the ground surface corresponding to the centreline of the embankment after the last consolidation phase (Figure 4, node A). The anisotropic creep model predicts a final settlement of 2.8 m, which is considerably larger that the one predicted by the isotropic creep model of about 2 m.

This general tendency of ACM to predict larger settlement than ICM is in agreement with other studies (Berengo et al. 2008). At this time excess pore pressures generated during construction were fully dissipated, therefore the effective stress is constant and the settlement rate of the final part of the curves is exclusively due to creep.

Figure 4b shows the excess pore pressure distribution immediately after construction at the symmetry axis. Both models predict the same qualitative distribution, which is also quantitatively correspondent until a depth of 6 m below ground level is reached.

At that point a discontinuity in the pre-overburden pressure occurs, and this is the reason for the deviation observed for larger depths. In particular the excess pore pressures predicted by ACM increase with depth at a larger rate than ICM. This is an effect of the different shape of the constitutive surfaces used: in ACM the ratio between deviatoric and volumetric component of the creep strain rate vector gives a stress distribution in agreement with Jaky's formula, whereas in ICM the ratio is larger.

This fact is to be expected when isotropic ellipses of Modified Cam Clay are assumed in combination with an

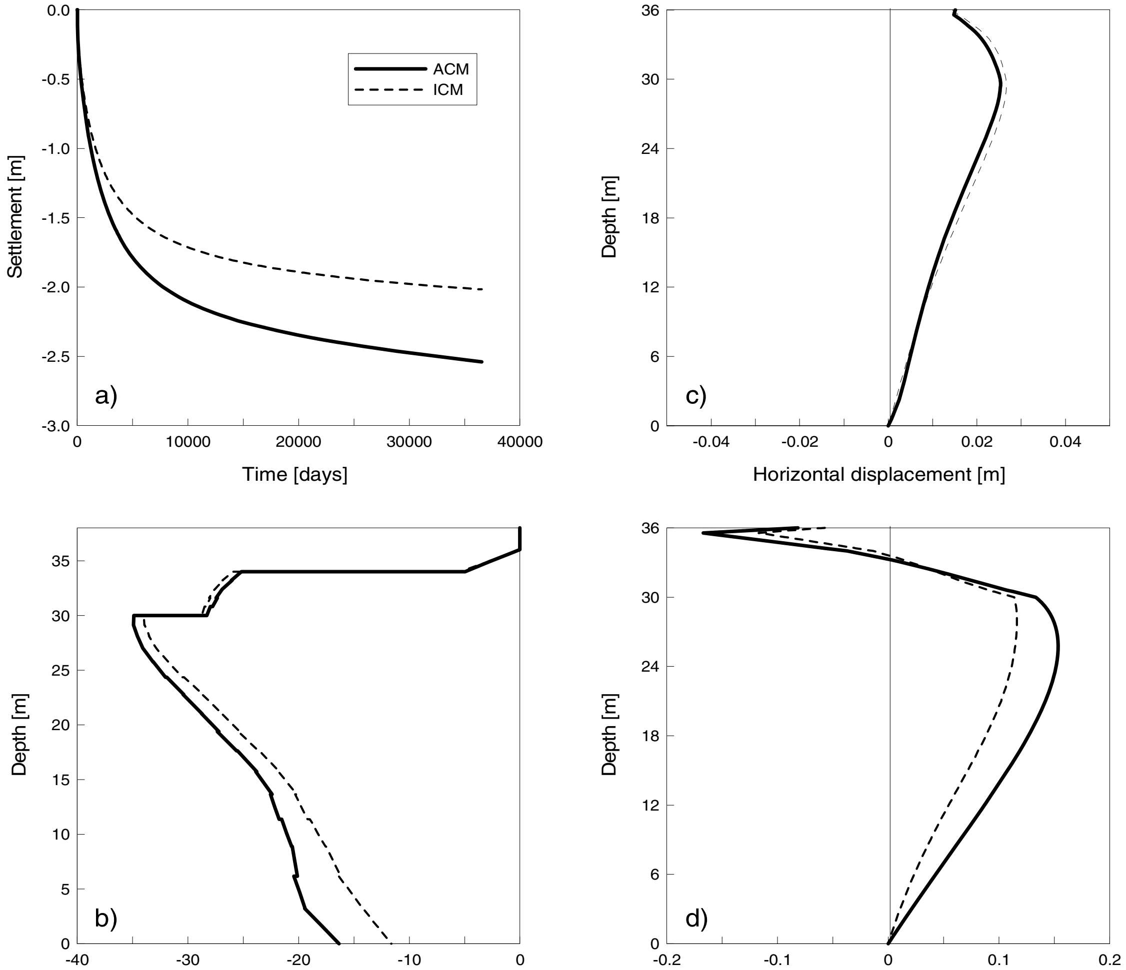

Figure 4. a) Vertical displacement of topmost point A; b) excess pore pressure after embankment completion (centreline); c) horizontal displacements at the embankment toe after construction; d) after 100 years of consolidation.

associated flow rule. The fact that in ACM no need for an unrealistic increase of the critical stress ratio is need, is already a remarkable improvement. Figure 4c shows the horizontal displacements underneath the toe of the embankment immediately after construction, whereas in Figure 4d horizontal displacements after 100 years' consolidation are shown. These results confirm the general tendency of ACM to predict larger horizontal displacements than the isotropic creep model. It is worth noting that the differences between ACM and ICM appear already immediately after construction, and those divergences tend to increase with consolidation time.

4 CONCLUSIONS

In this paper a newly developed anisotropic model (ACM) is used in a numerical simulation of a benchmark embankment.

ACM model is compared to a previously developed isotropic creep model. Results are presented in terms of displacements and pore pressures.

The comparison confirms the tendency of ACM to predict larger vertical and horizontal displacements both at the short term and long term conditions than the isotropic model. This is in agreement with recent studies in which the good numerical predictions of ACM were shown by comparing the numerical results with in situ measurements (Berengo et al. 2008).

It is worth highlighting that all the parameters involved in the anisotropic formulation have a clear physical meaning. Therefore, the improved predictions compared to the isotropic model are achieved at no further calibration cost. This feature, in the Authors' opinion, makes the ACM model very attractive from the point of view of engineering practice.

REFERENCES

Berengo, V., P. Simonini, M. Leoni, and P.A. Vermeer. 2008. Numerical modelling of the time-dependent behaviour of Venice lagoon soils. Paper read at 2nd Int. Workshop on Geotechnics of Soft Soils (IWGSS), at Glasgow.

Koskinen, M., R. Zentar, and M. Karstunen. 2002. Anisotropy of reconstituted POKO clay. Paper read at 8th Int. Symp. on Num. Models in Geomech. (NUMOG), at Rome.

Leoni, M., P.A. Vermeer, and M. Karstunen. 2008. Validation of a new anisotropic creep model. Paper read at 2nd Int. Workshop on Geotechnics of Soft Soils (IWGSS), at Glasgow.

Malvern, L.E. 1951. The propagation of longitudinal waves of plastic deformation in a bar of metal exhibiting a strain rate effect. Journal of Applied Mechanics 18 (2):203-208.

Perzyna, P. 1966. Fundamental problems in visco-plasticity. In Advances in applied mechanics, edited by G. Kuerti. New York: Academic Press.

Sekiguchi, H., and H. Ohta. 1977. Induced anisotropy and time dependency in clays. Paper read at 9th ICSMFE, at Tokyo.

Šukljie, L. 1957. The analysis of the consolidation process by the isotaches method. Paper read at 4th ICSMFE, at London.

Vermeer, P.A., and H.P. Neher. 1999. A soft soil model that accounts for creep. Paper read at Int.Symp. "Beyond 2000 in Computational Geotechnics", at Amsterdam.

Wheeler, S.J., A. Näätänen, M. Karstunen, and M. Lojander. 2003. An anisotropic elastoplastic model for soft clays. Canadian Geotechnical Journal 40 (2):403-418.